

# Telescopic resonators for large-volume TEM<sub>00</sub>-mode operation

D. C. HANNA, C. G. SAWYERS, M. A. YURATICH  
*Department of Electronics, University of Southampton, Highfield,  
Southampton SO9 5NH, UK*

*Received 20 May 1981; revised 30 June 1981*

A stable resonator incorporating a suitably adjusted telescope gives reliable operation of an Nd:YAG laser with a large-volume TEM<sub>00</sub> mode. The telescope adjustment is chosen to minimize the effect of focal length variations in the laser rod and at the same time ensures the optimum mode-selection properties of a confocal resonator. Simple approximations applied to the ray transfer matrices allow a detailed analysis of the resonator to be performed. This analysis yields simple design equations relating the mode spot sizes, resonator length, telescope magnification and defocusing, and diffraction losses. Experimental results show excellent agreement with the results of this analysis.

## 1. Introduction

By introducing a suitably adjusted telescope into a  $Q$ -switched Nd:YAG laser resonator we have been able to obtain reliable operation with a large-volume TEM<sub>00</sub> mode [1]. The basic principle behind the resonator design is that of choosing a telescope adjustment which compensates the thermal lensing in the laser rod (thus permitting a large spot size) and at the same time ensuring that the spot size is insensitive to fluctuations in focal length of the thermal lens. In order to illustrate the principles of the design, the discussion in [1] was given in terms of a simplified resonator in which the telescope and laser rod were assumed short compared to the overall resonator length and located close to one mirror. In fact, for accurate calculations in practical resonators these assumptions are too restrictive and in this paper we derive the necessary design equations taking into account the finite length of resonator occupied by the laser rod and telescope. However, before introducing the resonator analysis, we first briefly review some of the previous approaches to the operation of Nd:YAG lasers with high power and low beam divergence.

It has long been appreciated that, by compensating the thermal lens induced in solid-state laser rods, one can increase the TEM<sub>00</sub>-mode spot size and thus extract more energy in a diffraction-limited beam [2]. However, it is found that in general this compensation needs to be very precise if the mode size is to be comparable to typical laser rod diameters. Fluctuations in the focal length of this thermal lens (due to pump fluctuations) then lead to large spot-size fluctuations and thus unreliable performance of the laser. Steffen *et al* [3] pointed out this important effect of focal length fluctuations but also showed that stable resonators could be designed which are insensitive to these fluctuations. They referred to these resonators as 'dynamic stable resonators'. In one of their designs the resonator used two plane mirrors with the laser rod close to one mirror and the mirrors spaced by half the focal length of the rod's thermal lens. While this design did permit reproducible operation of an Nd:YAG laser with a large-volume TEM<sub>00</sub> mode, it suffered from an inconveniently long resonator. Another design made use of a short-radius convex mirror at one end of the resonator. This produces a large spot size at the other, concave, resonator mirror (the laser rod is located here) and allows a conveniently short resonator to be used. At about the same time Chesler and Maydan [4] also reported using a convex-concave resonator with a CW Nd:YAG laser. In a later paper Lörtscher *et al*. [5] gave further details of the performance of their convex-concave resonator and their results amply confirm that it is

possible to obtain reliable operation with a large-volume TEM<sub>00</sub> mode (up to 850 mJ fixed- $Q$  output was obtained from a pulsed Nd:YAG laser). However, the disadvantage of the convex-concave resonator is that the spot size is very small at the convex mirror and this effectively precludes its use in high-power  $Q$ -switched lasers. Thus  $Q$ -switched Nd:YAG lasers continued to be operated with conventional stable resonators which result either in a very multimode output when the full aperture of the laser rod is used or in a small output energy when apertured down to give TEM<sub>00</sub> operation.

An important advance was made with the application of unstable resonator techniques to the  $Q$ -switched Nd:YAG laser [6] since this allowed the extraction of a large energy in a low-divergence beam. The advantages of this were immediately apparent in such applications as harmonic generation. However, the diffraction-coupled output beam from an unstable resonator also has disadvantages associated with its non-uniform intensity profile [7]. These shortcomings have stimulated a search for other means (e.g. [8]) of producing high output energy in a low-divergence beam, but with a smooth intensity profile. Sarkies [9] reported using a telescope in an Nd:YAG resonator. An attractive feature of the telescope is that it allows easily controllable adjustment to compensate thermal lensing under varied pumping conditions. Although the output of his laser was not TEM<sub>00</sub>, Sarkies found that a good working compromise could be achieved with high output power and low beam divergence. We undertook our investigation of the telescopic resonator with a view to gaining a fuller understanding of its behaviour and in particular of seeing whether a large-volume TEM<sub>00</sub> mode could be obtained. In the course of our investigation we discovered that Steffen *et al.* [3] had suggested a telescopic resonator configuration as one means of realising a dynamic stable resonator. In their publications they make no mention of having used a telescopic resonator and yet it offers two advantages over their convex-concave resonator. These are (a) the easily controllable adjustment mentioned above and (b) the fact that it avoids the very small spot on the resonator mirror, and can therefore allow operation at the power levels typical of a  $Q$ -switched Nd:YAG laser. There is a third attractive feature, which applies to all dynamic stable resonators, namely that the diffraction losses produced by such resonators are the same as those of an equivalent symmetric *confocal* resonator. This result, which we derive in the Appendix, has not been referred to in earlier discussions of dynamic stable resonators. However, it has an important bearing on the problem of TEM<sub>00</sub> mode selection since it is the confocal geometry that provides the greatest degree of mode selectivity [10]. This feature, and the two advantages referred to above, have enabled us to obtain  $Q$ -switched TEM<sub>00</sub> outputs of greater than 100 mJ from an Nd:YAG laser with excellent reliability and without any damage problems.

## 2. Theory of the telescopic resonator

### 2.1. Preliminary remarks

First we write down the standard result [11] for the Gaussian-beam spot sizes  $w_1$  and  $w_2$  at the mirrors 1 and 2 (curvatures  $R_1$  and  $R_2$  respectively) of an empty resonator, as shown in Fig. 1. Expressed in terms of the  $g$  parameters,  $g_1 = 1 - L/R_1$  and  $g_2 = 1 - L/R_2$ , we have

$$\frac{\pi w_1^2}{\lambda} = L \left( \frac{g_2}{g_1(1 - g_1 g_2)} \right)^{1/2} \quad (1)$$

and

$$\frac{\pi w_2^2}{\lambda} = L \left( \frac{g_1}{g_2(1 - g_1 g_2)} \right)^{1/2} \quad (2)$$

We shall be concerned, in the discussion that follows, with resonators containing a laser medium which exhibits a thermally induced lensing behaviour, having a focal length  $f_R$ . At first we shall assume the laser medium to be adjacent to mirror 2, with the lens  $f_R$  incorporated in the curvature  $R_2$ . It can be seen from Equation 2 that the spot size,  $w_2$ , in the laser medium can be made arbitrarily large by an appropriate choice of  $R_1$ ,  $R_2$  and  $L$ . For example, with  $g_1 = 1$  (i.e.  $R_1$  plane), then as  $g_2 \rightarrow 1$ , so  $w_2 \rightarrow \infty$ . In practice, however, such a choice of parameters leads to a situation in which the spot size

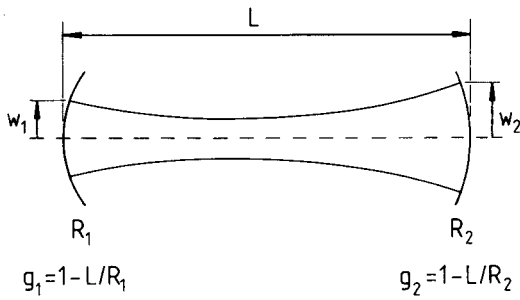


Figure 1 Empty resonator.

$w_2$  is extremely sensitive to the value of  $g_2$  and fluctuations in the value of  $f_R$  will cause variations of  $w_2$  which are too great to permit reliable selection of the TEM<sub>00</sub> mode. In fact, it can be shown from Equation 2 that the fractional change,  $dw_2/w_2$  of spot size due to a fractional change  $dg_2/g_2$  is given by

$$\frac{dw_2}{w_2} = \frac{1}{4} \frac{(2g_1g_2 - 1)}{(1 - g_1g_2)} \frac{dg_2}{g_2} \quad (3)$$

Thus, as  $g_1g_2 \rightarrow 1$ , the spot size  $w_2$  becomes sensitively dependent on  $g_2$  and hence  $f_R$ . However, if one chooses  $g_1g_2 = \frac{1}{2}$ , then Equation 3 shows that spot size  $w_2$  (but not  $w_1$ ) becomes insensitive to variations of  $g_2$ . This property was first exploited by Steffen *et al.* [3] in a resonator with two plane mirrors, with the laser rod close to mirror 2 (thus  $g_1 = 1, g_2 = 1 - L/f_R$ ), and the mirror separation  $L$  given by  $L = f_R/2$ , hence ensuring  $g_1g_2 = \frac{1}{2}$ . Substitution of  $g_1 = 1, g_2 = \frac{1}{2}$  in Equations 1 and 2 gives

$$w_1^2 = \frac{\lambda L}{\pi} \quad (4)$$

and

$$w_2^2 = \frac{2\lambda L}{\pi} = \frac{\lambda f_R}{\pi} \quad (5)$$

In this way, if  $f_R$  is large, then a large value of  $w_2$  can be obtained (one can always introduce a lens to compensate the thermal lens, thus making  $f_R$  effectively large). The disadvantage of this approach however is that the resonator is inconveniently long. It is worth noting here that this is actually a half-confocal resonator and an aperture placed at one mirror would therefore offer the ideal mode-selectivity characteristic of a confocal resonator (see the Appendix).

Another resonator design, which retains the condition  $g_1g_2 = \frac{1}{2}$ , but allows a short length  $L$ , involves choosing mirror 1 to be a very short-radius convex mirror, i.e.  $R_1$  negative and  $|R_1| \ll L$ , hence making  $g_1 \gg 1$ . Thus  $g_2$  is also positive but  $g_2 \ll 1$ , i.e.  $R_2$  corresponds to a concave reflector ( $R_2 > 0$ ) whose radius of curvature is slightly greater than  $L$ . An examination of Equations 1 and 2 shows that  $w_1^2 = (g_2/g_1)w_2^2$  and, since  $g_1g_2 = \frac{1}{2}$ , this gives

$$w_1^2 = \frac{1}{2g_1} w_2^2 \quad (6)$$

and

$$w_2^2 = \frac{2\lambda L}{\pi} g_1 \quad (7)$$

Comparing Equations 5 and 7 it can be seen that a large spot  $w_2$  can be produced in the laser medium (still assumed at mirror 2) with a short  $L$  provided  $g_1$  is large. However, Equation 6 shows that this

implies a very small  $w_1$ . Thus, although this resonator was successfully demonstrated [3, 5] for a fixed- $Q$  Nd:YAG laser, it would be unsuitable for a  $Q$ -switched laser.

The telescopic resonator which we now describe provides a compromise between the two resonator designs given above. To compare its performance with these two resonators we anticipate the results of our analysis and quote here the expressions for  $w_1$  and  $w_2$ , in the situation where (a) mirror 1 is plane, (b) the telescope, of magnification  $M$ , is assumed short and is placed close to the rod, which itself is at mirror 2, and (c) the telescope is adjusted to ensure insensitivity of spot size  $w_2$  to variations of  $f_R$ . Our analysis shows that  $w_1$  and  $w_2$  are given by

$$w_1^2 = \frac{L\lambda}{\pi} \quad (8)$$

and

$$w_2^2 = \frac{2L\lambda}{\pi} M^2. \quad (9)$$

Thus, compared with the long resonator described by Equations 4 and 5, for the same spot size  $w_2$ , the length of the telescopic resonator can be reduced by  $M^2$ , although this makes  $w_1$  smaller by a factor  $M$  than the corresponding value in the long resonator. On the other hand, when the telescopic resonator is compared with a convex-concave resonator of the same length and same spot size  $w_2$ , then  $g_1$  in Equation 7 takes the value  $M^2$  and it follows from Equation 6 that the spot size  $w_1$  in the telescopic resonator is  $M$  times larger than the spot size  $w_1$  on the convex mirror.

## 2.2. Derivation of an equivalent resonator for the telescopic resonator

In making these preliminary remarks about the telescopic resonator we chose a simplified resonator as an illustration. In practice, the simplifications made, such as assuming a short telescope and short laser rod, are too sweeping for accurate calculation. We now consider a telescopic resonator, shown in Fig. 2, for which the simplifying assumptions have been dropped. Both mirrors are assumed curved and the resonator contains a telescope of magnification  $M = -f_2/f_1$  and a lens, focal length  $f_R$ , representing the laser rod. The length  $L$  now refers to the length of that part of the resonator occupied by the contracted beam. The telescope lenses are spaced by  $d + \delta$  where  $d = f_1 + f_2$  and  $\delta$  is referred to as the telescope defocusing<sup>†</sup>. The centre of the laser rod is spaced an optical distance  $l_2$  from the second telescope lens (focal length  $f_2$ ), and the mirror 2 is spaced a further optical distance  $l_1$  from the rod centre.

We shall find it convenient to treat a mirror of curvature  $R$  as a plane mirror with an adjacent lens of focal length  $R$  in front of it. This approach has the merit of allowing the resonator properties to be calculated in terms of the single-pass, ray-transfer matrix elements, where a single pass takes one from the left-hand plane mirror (plane 1) to the right-hand plane mirror (plane 2).

The analysis is aimed at finding simplified expressions for the spot sizes  $w_1$ ,  $w_2$ , and in particular at finding the value of  $\delta$  which makes  $w_2$  insensitive to variations of  $f_R$ . Our procedure is first to consider the case where mirror 2 is in fact adjacent to the rod, and the rod is short, so  $l_1 = 0$ , and where the rod is in the focal plane of the telescope objective (lens  $f_2$ ) so  $l_2 = f_2$ . This gives compact and exact results which exhibit the main features of the telescopic resonator. It is then possible to relax the above restrictions, and introduce arbitrary spaces  $l_2$  and  $l_1$ ; the formulae are more complex, and we discuss their approximations.

It is readily shown that the ray matrix [11] of the telescope  $f_1, d + \delta, f_2$  is

$$\begin{bmatrix} M - \frac{\delta}{f_1} & d + \delta \\ \frac{\delta}{f_1 f_2} & \frac{1}{M} - \frac{\delta}{f_2} \end{bmatrix} \quad (10)$$

<sup>†</sup>Strictly, if the resonator length is to remain fixed as the telescope defocusing is varied,  $L$  should be replaced by  $L - \delta$ . We shall ignore this small correction however as it can be shown that it has a negligible effect.

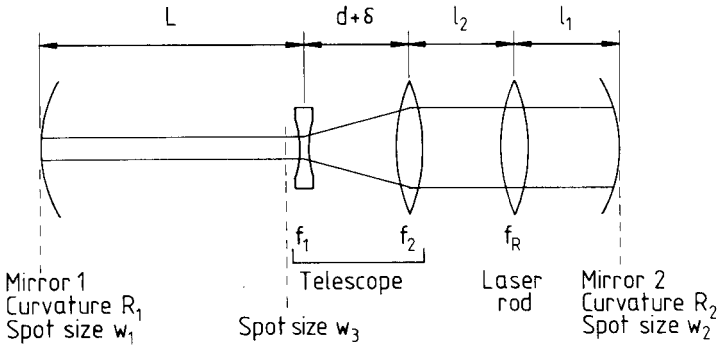


Figure 2 The telescopic resonator.

This matrix may be factorized *exactly* into a space  $-f_1$ , a 'thin telescope', a thin lens  $f_T$  and a space  $-f_2$ :

$$\begin{bmatrix} 1 & -f_2 \\ 0 & 1 \end{bmatrix} \begin{bmatrix} 1 & 0 \\ -1/f_T & 1 \end{bmatrix} \begin{bmatrix} M & 0 \\ 0 & 1/M \end{bmatrix} \begin{bmatrix} 1 & -f_1 \\ 0 & 1 \end{bmatrix} \quad (11)$$

where the ray matrix of the thin telescope is

$$\begin{bmatrix} M & 0 \\ 0 & 1/M \end{bmatrix} \quad (12)$$

and the thin lens' focal length is

$$\frac{1}{f_T} = \frac{\delta}{f_2^2}. \quad (13)$$

The effect of the thin telescope is to expand the spot size of the beam by a factor  $M$  and to reduce the beam curvature by a factor  $M$ , so that there is a beam discontinuity in its plane. Note that the telescope defocusing is described by a single element, the lens  $f_T$ . Equation 11 provides a key to the telescopic resonator. It shows that the resonator is exactly equivalent to one containing the following sequence of elements: a lens  $R_1$ , a space  $L'$ , where

$$L' = L - f_1, \quad (14)$$

the thin telescope, a lens pair  $f_T, f_R$  separated by a space  $l_2 - f_2$ , a space  $l_1$  and a lens  $R_2$ . By choosing  $l_2 = f_2$ , the lenses  $f_T$  and  $f_R$  are made adjacent and form a compound lens. Since  $1/f_T$  is proportional to  $\delta$ , the compound lens has an adjustable focal length, which can be used to precisely compensate its rod lens component  $f_R$ . By making the further restriction that  $l_1 = 0$ , we have a compound lens of focal length  $R'_2$ , where

$$\frac{1}{R'_2} = \frac{1}{f_T} + \frac{1}{f_R} + \frac{1}{R_2}. \quad (15)$$

The restricted resonator with  $l_2 = f_2$  and  $l_1 = 0$  is depicted in Fig. 3. Its *exact* single-pass ray matrix is

$$\begin{bmatrix} A & B \\ C & D \end{bmatrix} = \begin{bmatrix} G_1 & ML' \\ -\frac{(1-G_1G_2)}{ML'} & G_2 \end{bmatrix} \quad (16)$$

where the  $G$  parameters are given by

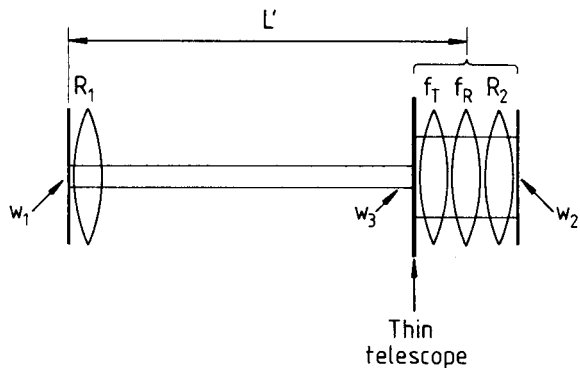


Figure 3 Equivalent telescopic resonator with both thin telescope and laser rod located at mirror 2.

$$G_1 = M \left( 1 - \frac{L'}{R_1} \right) \tag{17a}$$

$$G_2 = \frac{1}{M} \left( 1 - \frac{M^2 L'}{R_2'} \right) \tag{17b}$$

With the help of these equations one can express spot sizes in either of the commonly used ways, namely in terms of  $A, B, C$  and  $D$ , or in terms of  $G_1$  and  $G_2$ . The latter are particularly convenient for a discussion of resonator stability. The  $G$  parameters defined here are a generalization of the usual parameters  $g_1$  and  $g_2$  for an empty resonator, and if we let  $M = 1$ , i.e. if the telescope is removed, then  $G_1 \rightarrow g_1 = 1 - L/R_1$  and  $G_2 \rightarrow g_2 = 1 - L/R_2$ .

As shown by Baues [12] the spot sizes are given by

$$\frac{\pi w_1^2}{\lambda} = \left( -\frac{BD}{AC} \right)^{1/2} \tag{18a}$$

$$\frac{\pi w_2^2}{\lambda} = \left( -\frac{AB}{CD} \right)^{1/2} \tag{18b}$$

It is convenient to normalize the spot sizes to  $\lambda L'$ , bearing in mind that typically  $L'$  is approximately equal to the length  $L$  of resonator occupied by the contracted beam. Thus the normalized spot sizes  $W$  are

$$W_1 = \left( \frac{\pi w_1^2}{\lambda L'} \right)^{1/2} = \left[ \frac{M^2 G_2}{G_1 (1 - G_1 G_2)} \right]^{1/4} \tag{19a}$$

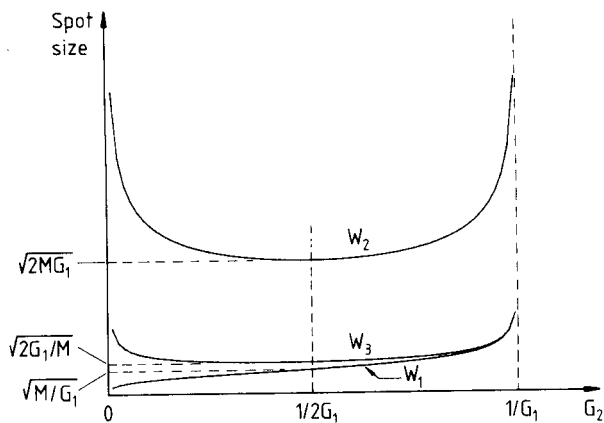


Figure 4 Normalized spot sizes  $W_1, W_2$  and  $W_3$  versus  $G_2$  for fixed values of  $M$  and  $G_1$ .

and

$$W_2 = \left( \frac{\pi w_2^2}{\lambda L'} \right)^{1/2} = \left[ \frac{M^2 G_1}{G_2(1 - G_1 G_2)} \right]^{1/4} \quad (19b)$$

and at the entrance to the telescope, i.e. at the lens  $f_1$ , the spot size is

$$W_3 = \left( \frac{\pi w_3^2}{\lambda L'} \right)^{1/2} = W_2/M. \quad (19c)$$

Fig. 4 shows the behaviour of the spot sizes  $W_1$ ,  $W_2$  and  $W_3$  as a function of  $G_2$  with  $G_1$  and  $M$  fixed. From Equations 15 and 17, these curves also represent the dependence of spot sizes on telescope defocusing  $\delta$ . A number of important results are indicated in this figure. First we note that the spot size  $W_2$  is insensitive to variations of  $G_2$  when  $G_2 = 1/2G_1$ , i.e. when  $G_1 G_2 = \frac{1}{2}$ , and this is therefore the desired operating point. In fact, a comparison of Equation 19b with Equation 2 is enough to show that the earlier condition  $g_1 g_2 = \frac{1}{2}$  now becomes  $G_1 G_2 = \frac{1}{2}$ . The spot sizes  $W_2$ ,  $W_3$  and  $W_1$  for  $G_1 G_2 = \frac{1}{2}$  are indicated in Fig. 4 as  $(2MG_1)^{1/2}$ ,  $(2G_1/M)^{1/2}$  and  $(M/G_1)^{1/2}$  respectively. Thus the ratio of spot sizes,  $W_2/W_1$ , is  $G_1\sqrt{2}$ , an important quantity to bear in mind when considering the question of damage to components in the contracted beam. For the particular case where mirror 1 is plane,  $G_1$  then has the value  $M$  and the normalized spot sizes  $W_2$ ,  $W_3$  and  $W_1$  are  $M\sqrt{2}$ ,  $\sqrt{2}$  and 1 respectively, a result previously quoted in Equations 8 and 9. From Fig. 4 it can be seen that the minimum of  $W_2$  is quite flat and from Equation 19b one can show that a 10% change of  $G_2$  about the operating point  $G_1 G_2 = \frac{1}{2}$  (i.e.  $G_2$  varying from  $0.4/G_1$  to  $0.6/G_1$ ) causes only a 1% increase in  $W_2$ . The spot size  $W_1$  does however vary and  $(dW_1/dG_2)_{G_1 G_2 = 1/2} = (MG_1)^{1/2}$ . The figure also indicates that as one approaches the boundaries of stable operation (at  $G_2 = 0$  and  $G_1 G_2 = 1$ ) the spot size  $W_2$  diverges, whereas the spot size  $W_1$  goes to zero as  $G_2 \rightarrow 0$  and diverges as  $G_1 G_2 \rightarrow 1$ . In Section 2.3 we discuss the choice of  $\delta$  which optimizes  $G_2$  and hence the performance of the telescopic resonator.

The stability behaviour can be illustrated with reference to the  $G_1 G_2$  plane, of which the positive quadrant is shown in Fig. 5. The stable region is enclosed by the  $G_1$  and  $G_2$  axes and the hyperbola  $G_1 G_2 = 1$ . The locus of ideal adjustment  $G_1 G_2 = \frac{1}{2}$  is also a hyperbola, passing essentially through the centre of the stable region. An empty resonator with mirror 1 plane ( $G_1 = 1$ ) and mirror 2 concave with  $R_2 > L$  (hence  $G_2 > 0$ ) is represented by a point on the line PQ. The point U represents the half-confocal resonator, Q the plane-plane resonator. If a thin telescope of magnification  $M$  is inserted adjacent to mirror 2 in the resonators represented by the line PQ, they will then be represented by points on the line RS, with the point S corresponding to the plane-plane resonator and the point V corresponding to the ideal operating point. As the magnification  $M$  is increased, so the range of values of  $G_2$  for stable operation is decreased.

Having discussed the properties of the telescopic resonator with the particular choice  $l_2 = f_2$  and  $l_1 = 0$ , we now consider arbitrary spacings. Whereas the first case allowed us to derive exact and compact expressions, in the case of arbitrary spacings the exact expressions are very cumbersome. Exact results can, of course, be obtained on a computer, but our aim here is to show that in fact the expressions derived above remain quite adequate for practical spacings.

Any ray matrix can be put into the form of Equation 16, and with appropriate parameters  $G'_1$ ,  $G'_2$ ,  $L''$  say, all the discussion relating to Fig. 4 and Equations 18 and 19 for the spot sizes still applies. However, the expressions for  $G'_1$ ,  $G'_2$ ,  $L''$  (and hence  $A$ ,  $B$ ,  $C$  and  $D$ ) in terms of the physical resonator parameters will now differ from the  $G_1$ ,  $G_2$  and  $L'$  of Equations 14 and 17. From Equation 18 it is seen that the spot sizes vary as  $B^{1/4}$ , and so any small error in  $B$  will be insignificant. On the other hand, the spot sizes vary as  $1/C^{1/4}$  and  $1/D^{1/4}$ , and so errors in  $C$  or  $D$  will have a large effect on the spot sizes, since the limits of the stable region are defined by  $C = 0$  and  $D = 0$ . We conclude that when making approximations,  $C$  and  $D$  need more care than  $B$ ;  $A$  can be regarded as a derived parameter since  $AD - BC = 1$ .

Consider first the case where  $l_2 \neq f_2$ . The matrix elements are readily determined, and may be put into the form:

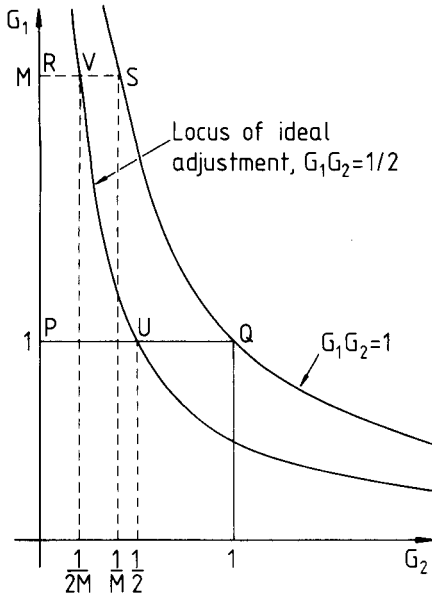


Figure 5 Stability diagram. The line PQ represents stable empty resonators with mirror 1 plane ( $G_1 = 1$ ). The line RS represents stable resonators with thin telescope adjacent to mirror 2, and mirror 1 plane ( $G_1 = M$ ).

$$A = M \left(1 - \frac{\Delta}{f_T}\right) \left\{1 - \frac{L'}{R_1} \left[1 + \frac{\Delta}{M^2 L' (1 - \Delta/f_T)}\right]\right\} \quad (20a)$$

$$B = ML' \left(1 - \frac{\Delta}{f_T}\right) \left[1 + \frac{\Delta}{M^2 L' (1 - \Delta/f_T)}\right] \quad (20b)$$

$$C = -\frac{1}{ML'} \left(1 - \frac{\Delta}{f}\right) \left[1 - M \left(1 - \frac{L'}{R_1}\right) \left(\frac{1}{M} - \frac{ML'}{R_2''}\right)\right] \quad (20c)$$

$$D = \frac{1}{M} \left(1 - \frac{\Delta}{f}\right) \left(1 - \frac{M^2 L'}{R_2''}\right) \quad (20d)$$

where

$$\Delta = l_2 - f_2 \quad (21a)$$

$$\frac{1}{f} = \frac{1}{f_R} + \frac{1}{R_2} \quad (21b)$$

$$\frac{1}{R_2''} = \frac{1}{f_T} + \frac{1}{f - \Delta} \quad (21c)$$

In practice,

$$|\Delta| \ll |f|, |f_T|, M^2 L' \quad (22)$$

or can be made so by design. Thus the term  $\Delta/f$  can be dropped from Equation 20d, giving

$$D = G_2' \approx \frac{1}{M} \left(1 - \frac{M^2 L'}{R_2''}\right) \quad (23a)$$

Note that the limit of the stable region defined by  $D = 0$  is still an *exact* function of  $R_2''$ , and hence of the defocusing  $\delta$ . Turning to Equation 20c, then with  $G_2'$  defined by Equation 23a and by comparison with element  $C$  in Equation 16, it is seen that a suitable choice of  $G_1'$ , and hence of  $A$ , is



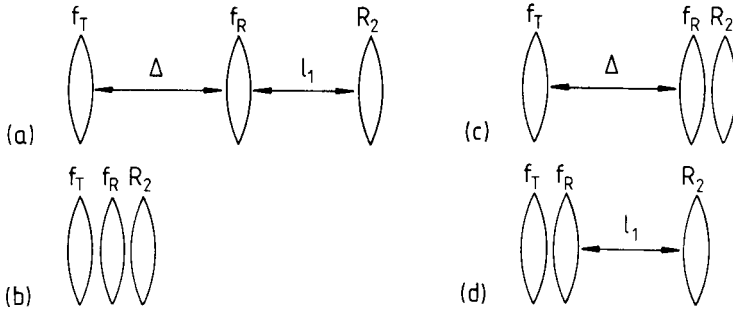


Figure 6 Various cases of resonator lens combinations.

$$A = G'_1 \simeq M \left( 1 - \frac{L'}{R_1} \right). \quad (23b)$$

As with  $D$ , this choice gives the zero of element  $C$  exactly.  $B$  can be approximated by dropping the terms  $\Delta/f_T$  and  $\Delta/M^2 L' (1 - \Delta/f_T)$ , giving

$$B \simeq M L', \quad L'' = L'. \quad (23c)$$

(It is seen that we have effectively approximated  $A$  in the same way as  $B$ .) To summarize, we have found that by making the assumptions of Equation 22, our earlier treatment of the telescopic resonator comes through with the one change, of  $R'_2$  to  $R''_2$ . Moreover, as  $|\Delta| \ll |f|$  from Equation 22, we can generally ignore the change, and use the original Equations 15–17.

Fig. 6a shows the actual resonator lenses  $f_T$ ,  $f_R$  and  $R_2$  and their spacings  $\Delta$  and  $l_1$ . Figs. 6b and c respectively depict the special case  $\Delta = l_1 = 0$  treated earlier, and the case  $\Delta = 0, l_1 = 0$  just examined. The last case we wish to examine,  $\Delta = 0, l_1 \neq 0$ , is shown in Fig. 6d. By comparing with Fig. 6c it is apparent that Equation 20 can again be used, but with the changes  $1/f_T \rightarrow 1/f_T + 1/f_R$ ,  $\Delta \rightarrow l_1$ , and  $1/f \rightarrow 1/R_2$ . The inequalities corresponding to Equation 22 are  $l_1 \ll |R_2|$ ,  $|1/f_R + 1/f_T|^{-1}$ ,  $M^2 L'$ , and these again are satisfied in practice. Hence the only change from the first expressions (Equations 15–17) is that  $R'_2$  is replaced by  $R''_2$ , where

$$\frac{1}{R''_2} = \frac{1}{f_T} + \frac{1}{f_R} + \frac{1}{R_2 - l_1}. \quad (24)$$

Again  $l_1$  can often be omitted, for example in the instance where mirror 2 is plane. However, whereas  $\Delta$  is the difference of two comparable lengths,  $\Delta = l_2 - f_2$ , and so always tends to be small,  $l_1$  may give a significant correction in Equation 24, and hence to the predicted defocusing  $\delta$  in  $f_T$ .

### 2.3. Choice of resonator parameters and telescope defocusing

In the previous section we have shown that the telescopic resonator can be characterized by the values  $G_1$  and  $G_2$  of its equivalent resonator containing a thin telescope. We concluded that the telescopic resonator should be adjusted so that its equivalent resonator satisfies the condition  $G_1 G_2 = \frac{1}{2}$ . This can be achieved by adjusting the telescope defocusing  $\delta$ , since this determines  $f_T$  (through Equation 13), hence  $R'_2$  (through Equation 15) and finally  $G_2$  (through Equation 17b). Thus, with  $G_1 G_2$  put equal to  $\frac{1}{2}$ , we find that  $\delta_{\text{opt}}$  is given by

$$\delta_{\text{opt}} = f_2^2 \left[ \frac{1}{M^2 L'} \left( 1 - \frac{M}{2G_1} \right) - \frac{1}{f_R} - \frac{1}{R_2} \right] = f_2^2 \left[ \frac{1}{2M^2 L'} \left( \frac{1 - 2L'/R_1}{1 - L'/R_1} \right) - \frac{1}{f_R} - \frac{1}{R_2} \right]. \quad (25)$$

Once the resonator parameters  $M$ ,  $f_2$ ,  $L$ ,  $R_1$  and  $R_2$  have been chosen and  $f_R$  is known, then  $\delta_{\text{opt}}$  can be calculated from Equation 25. The value of  $f_R$  depends on the operating conditions (repetition rate and pump energy) and provided its dependence is known one can then calculate the necessary changes of  $\delta_{\text{opt}}$  for changed operating conditions. The effect of a change in  $f_R$  is to change  $R'_2$  and hence  $G_2$ .

This simply translates the curves in Fig. 4 parallel to the  $G_2$  axis. A change of  $\delta$  has exactly the same effect since it changes  $f_T$  and hence  $R'_2$ . Thus the curves of Fig. 4 also indicate the dependence of spot sizes on telescope defocusing. This behaviour provides an experimental means of identifying whether one is operating at the optimum point. As  $G_1G_2$  is made to depart from its optimum value by changing the telescope defocusing it is found that the laser output energy drops and the beam quality degrades. This drop in performance shows a symmetric behaviour on either side of the optimum so that, for example, a plot of output energy versus  $\delta$  will exhibit a rather flat maximum and this can be used to locate  $\delta_{\text{opt}}$  roughly. Fine adjustment of  $\delta$  is usually then required for final optimization of performance.

We have indicated how  $\delta_{\text{opt}}$  can be calculated once the resonator parameters are chosen. We now consider some of the factors that influence the choice of these parameters. Obviously one cannot give here an all-embracing strategy for the optimum selection of these parameters since they are influenced by the operating conditions of the laser. For example, if the laser is  $Q$ -switched then it is likely that damage limitations of components in the contracted beam will be a major factor in deciding the energy to be extracted. This influences the choice of spot diameter in the laser rod. Under fixed- $Q$  conditions quite different considerations apply and the maximum spot size in the laser rod may then be determined by inhomogeneities caused by thermally induced birefringence [13]. If damage is the main limitation then one must seek a compromise between the convenience of a short resonator with its greater risk of damage and the inconvenience of a long resonator. This choice can be illustrated most clearly by considering a resonator with mirror 1 plane ( $G_1 = M$ ) and, since  $G_1G_2 = \frac{1}{2}$ , then  $G_2 = 1/2M$ , for which Equations 19a and b yield

$$w_1^2 = L'\lambda/\pi \quad (26)$$

and

$$w_2^2 = \frac{2L'\lambda M^2}{\pi} \quad (27)$$

Equation 27 shows that for a given  $w_2$ , the smaller one makes  $L'$  (by choosing a larger  $M$ ), the smaller is  $w_1$ . This increases the risk of damage due to the higher energy density and also, since the resonator is shorter, due to the shorter pulse duration. The damage limitations of dielectric coatings have led us to use an uncoated plane parallel plate of fused silica as the reflector for the contracted beam and this then serves as the output mirror.

The laser used in our experiments has a 75 mm  $\times$  9 mm Nd:YAG rod pumped by twin flash-lamps. We have operated this laser with TEM<sub>00</sub> spot diameters ( $2w_2$ ) up to 5 mm and it is likely that at repetition rates of less than 10 Hz, where thermally induced birefringence effects remain small [13], even larger spot sizes would be feasible. A typical set of resonator parameters as used in most of our work is as follows:  $L = 0.34$  m,  $M = 4$ ,  $f_1 = -0.05$  m (hence  $f_2 = 0.20$  m and  $d = 0.15$  m),  $l_2 = 0.25$  m,  $l_1 = 0.51$  m. Hence  $L' = 0.39$  m (from Equation 14),  $w_1 = 0.36$  mm (from Equation 26) and  $w_2 = 2.1$  mm (from Equation 27). The overall optical length of the resonator was 1.25 m and when the output energy  $E$  was  $\sim 100$  mJ the pulse duration  $\tau$  was measured to be 30 ns (FWHM). The peak intensity at the resonant reflector is then  $2E/\pi w_1^2 \tau = 2E/\lambda \tau L'$ , which for our parameters gave a value of  $1.6 \text{ GW cm}^{-2}$ . This is to be compared with values for the damage threshold of Spectrosil B when subjected to 10 ns pulses of  $1.06 \mu\text{m}$  radiation, namely  $5 \text{ GW cm}^{-2}$  [14]. The spot size  $w_3$  at the small lens of the telescope is, according to Equation 19c,  $\sqrt{2}$  greater than  $w_1$ . We have found that AR coatings on this lens are liable to damage and an uncoated lens of BK7 is therefore used. Apart from the use of uncoated optics in the contracted beam we have not made any serious attempt to optimize the damage threshold. Our laser has been operated with the resonator parameters listed above, producing  $Q$ -switched outputs of  $\sim 100$  mJ for  $\sim 10^6$  shots, so far with no sign of damage<sup>†</sup>. To optimize the damage threshold one would need to examine the various trade-offs, such as increasing the resonator length, decreasing the magnification, etc., and Equations 19a and 19b provide the basis on which to carry out this

<sup>†</sup>In deliberate attempts to induce damage we found that a small damage speck could be produced on the Spectrosil flat when the laser output energy reached 150–170 mJ.

optimization analytically. The simplicity of the design equations (Equations 13–19 and 25) makes their use very straightforward.

For the exact calculation of spot sizes one needs to know  $f_R$ . Using a He–Ne laser we have measured the mean focal length of the laser rod for various average pump input powers  $P$  (kW) and find that the focal length (in metres) is given by  $f_R = 2.7/P$ . We have assumed that this measured value of focal length corresponds to the actual value which prevails at the time when laser oscillation occurs. Thus we assume that transient focal length variations during pumping, such as observed by Baldwin and Riedel [15], are small compared to the mean focal length. This assumption appears to be valid for our operating conditions since the observed changes of  $\delta_{\text{opt}}$  (i.e. the necessary telescope readjustment) for given changes of pump power  $P$  were found to agree with those predicted by Equation 25 with  $f_R$  put equal to  $2.7/P$  and both  $1/R_1$  and  $1/R_2$  put equal to zero, i.e.

$$\delta_{\text{opt}} = f_2^2 \left[ \frac{1}{2M^2 L'} - \frac{1}{f_R} \right]. \quad (28)$$

This equation therefore provides a very simple prescription for change of telescope adjustment with change in average pump power. Typically we have operated the laser with a modest repetition rate ( $\sim 8$  Hz) and  $f_R \sim 4$  m. It should be noted that under conditions involving a high average output power from the laser (such as where a high repetition rate is used) it is possible for the Pockels cell to contribute noticeable negative lensing due to absorption of the laser radiation. This was noticed by observing that  $\delta_{\text{opt}}$  shifted in value when the Pockels cell was added to the resonator (between the laser rod and mirror 2) while it was operating under fixed- $Q$  conditions with 350 mJ TEM<sub>00</sub> output at 18 Hz repetition rate. The effects of such a lens, of focal length  $f_P$ , can be included in the foregoing analysis simply by adding  $1/f_P$  to the term  $1/f_R$  in Equations 15, 25 and 28. From the observed shift of  $\delta_{\text{opt}}$ , the value of  $f_P$  was estimated from Equation 28 as  $-20$  m. This is consistent with the value calculated (following [16]) by assuming an absorption coefficient in the KD<sup>+</sup>P Pockels cell corresponding to 95% deuteration [14]. However under our typical operating conditions (100 mJ output at 8 Hz) the Pockels cell lensing was not significant.

An experimental check on the alignment tolerances of the laser mirrors was made by observing the mirror tilt required to reduce the output energy by 20% from its optimum value. This reduction was produced by a  $\sim 0.3$  mrad tilt of mirror 1 and a  $\sim 0.08$  mrad tilt of mirror 2. Beam quality was not noticeably altered by this amount of tilt. These angles correspond to around one third of the calculated divergence (half-angle) of the beam incident on the respective mirrors. This confirms the expected result that the alignment tolerance of the mirror in the expanded beam should be tighter by a factor  $\sim M$  (i.e. 4 in this case).

We conclude this section by showing, in Fig. 7, the calculated spot sizes  $w_1$ ,  $w_2$  and  $w_3$  versus telescope defocusing  $\delta$  for the typical set of resonator parameters quoted earlier. The calculations have been made in two ways: (a) using exact ray-transfer matrices throughout, shown as full curves in Fig. 7, and (b) using Equations 14–19, shown as broken curves. The excellent degree of accuracy obtainable from the approximate equations is apparent.

### 3. Choice of mode-selecting aperture

The TEM<sub>00</sub> mode is selected by means of a circular aperture which is accurately centred on to the laser axis by micrometer adjustment. One can in principle use an aperture either in the contracted or expanded beam (provided the aperture size is appropriate, see Appendix) but we have chosen the latter for two reasons (a) for convenience, since the larger aperture is less liable to damage, and (b) the resonator is designed to minimize variations in spot size of the expanded but not of the contracted beam.

The aperture introduces round-trip diffraction losses  $L_{00}$  and  $L_{10}$  respectively for the TEM<sub>00</sub> and TEM<sub>10</sub> modes. The degree of mode selection (i.e. ratio of TEM<sub>00</sub> power to TEM<sub>10</sub> power) resulting

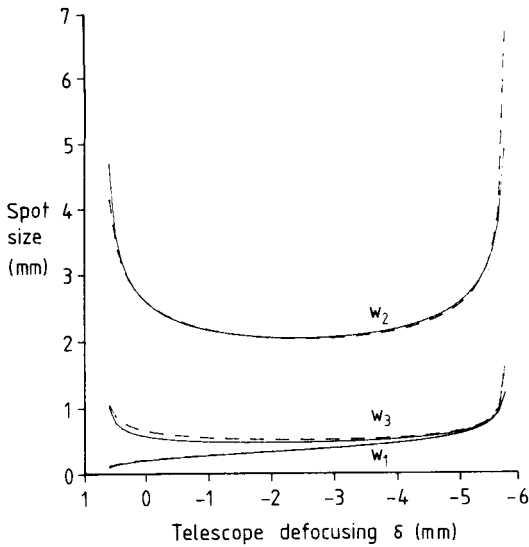


Figure 7 Calculated spot sizes versus telescope defocusing for the typical resonator parameters indicated in the text. The full curves were obtained using exact ray-transfer matrices throughout and the broken curves using the approximate Equations 14–19.

from  $q$  round trips is thus given by<sup>†</sup>:  $[(1 - L_{00})/(1 - L_{10})]^q$ . The losses  $L_{00}$  and  $L_{10}$  can be found exactly using the results of Li [10] provided the aperture (which is assumed to be the dominant cause of diffraction loss) is located at a resonator mirror. First however we consider a rough estimate of loss which can be made by calculating that fraction of the power in the Gaussian beam (spot size  $w$ ) intercepted by an aperture of diameter  $2a$ . For a  $TEM_{00}$  mode this is given by (see e.g. [17])

$$L_{00} = \exp(-2a^2/w^2) \tag{29}$$

and for a  $TEM_{10}$  mode, by

$$L_{10} = \left(1 + \frac{2a^2}{w^2}\right) \exp(-2a^2/w^2). \tag{30}$$

Like Lörtscher *et al.* [15] we have used an aperture size such that  $a$  is nominally equal to  $1.5 w$ , thus giving  $L_{00} = 0.011$  and  $L_{10} = 0.061$ , according to Equations 29 and 30. If one considers a typical  $Q$ -switched Nd:YAG laser where  $q$  may be  $\sim 35$ , the above values of loss would then imply  $[(1 - L_{00})/(1 - L_{10})]^q \approx 6$ .

One thing that is apparent from this calculation is that the degree of mode selection is sensitively dependent on the values of  $L_{00}$  and  $L_{10}$ . In the Appendix we show how an exact calculation of  $L_{00}$  and  $L_{10}$  can be made, using an equivalence relation between the actual resonator used and a symmetric resonator for which exact diffraction-loss calculations have been performed [10]. The result from the Appendix is quoted here, namely, that a round trip of the telescopic resonator, starting from the aperture (diameter  $2a$ , located at mirror 2 in the expanded beam) produces the same diffraction loss as a single pass through a *confocal* symmetric resonator of Fresnel number  $a^2/[2\lambda M^2 L'(1 - L'/R_1)]$ , where  $L' = L - f_1$ , (Equation 14). Li [10] has shown that the confocal geometry provides the greatest mode selectivity, and it is a useful feature of the telescopic resonator that it is able to exploit this property. From Li's paper (his Fig. 8) one can see that for a  $TEM_{00}$  loss of 0.01, the  $TEM_{10}$  loss is 0.12, thus giving a value for  $[(1 - L_{00})/(1 - L_{10})]^q$  of  $\sim 60$  for  $q = 35$ .

Despite this large selectivity it must be borne in mind that the mode selection is a sensitive function of  $L_{00}$  and  $L_{10}$  and hence of aperture size. It is therefore advisable, in selecting the aperture size, to have

<sup>†</sup>The analysis leading to this expression ignores possible mode distortion effects due to non-uniform saturation of the spatial (radial) gain distribution. However, for most of the pulse build-up, such saturation effects are in fact absent.



Figure 8 Sequence of burns on photographic paper. These were taken at 4 m from the resonant reflector, at an output energy of  $\sim 100$  mJ and a repetition rate of 8 Hz.

available a range of closely spaced aperture sizes so that one can find in practice which gives the most satisfactory performance. Using the parameters already quoted for our resonator and the aperture diameter  $2a = 6.25$  mm, the above expression for Fresnel number yields the value 0.74. With this Fresnel number, Li's calculations give round-trip losses for our resonator of  $L_{00} = 0.008$  and  $L_{10} = 0.10$ , thus giving a generous degree of mode selection over the 35 or so round trips when  $Q$ -switched. The very small diffraction loss for the TEM<sub>00</sub> mode suggests that little or no diffraction ring structure would be visible in the output beam since the mode is only very slightly truncated. This is indeed the case and Fig. 8 shows a sequence of burn patterns on photographic film. These were taken at 4 m from the output resonant reflector. Fig. 9 shows the TEM<sub>00</sub> mode intensity profile as observed on a diode array, confirming the smooth, structureless profile indicated by the burn patterns. Spot sizes measured using the diode array agree within experimental accuracy with TEM<sub>00</sub> spot sizes predicted by our analysis.

#### 4. Conclusion

We have shown that a telescopic resonator can provide a reliable means of generating a large-volume TEM<sub>00</sub> mode in a Nd:YAG laser, permitting  $Q$ -switched operation at the 100 mJ level. An analytical

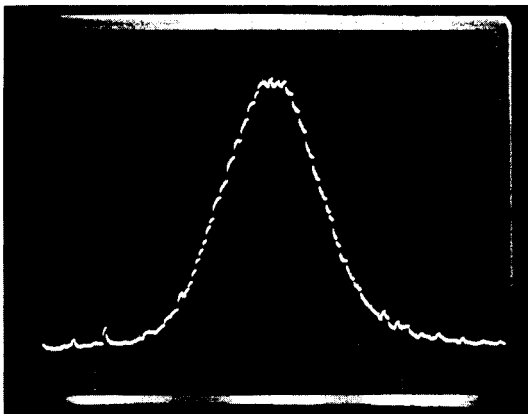


Figure 9 Beam profile as monitored by a diode array.

description of this type of resonator has been developed which reduces to a few simple design equations. We have found that these equations describe the experimentally observed behaviour with a degree of completeness and accuracy beyond what was expected. This indicates that a very thorough design calculation could be made, e.g. to maximize output energy while keeping clear of damage problems, and the results of such a calculation could be trusted with confidence. It is expected that a similar exercise could be extended to other optically pumped solid-state lasers, notably Nd-doped glass and ruby.

### Acknowledgements

This work has been supported by a grant from the Science Research Council and one of us (CGS) wishes to acknowledge support from the SRC and UKAEA (Culham Laboratory) in the form of a Case Studentship. We also wish to acknowledge helpful discussions with Dr P. H. Sarkies and assistance from Mr A. J. Berry.

### Appendix. Calculation of diffraction loss for TEM<sub>00</sub> and TEM<sub>10</sub> modes

We consider a general resonator represented, as in Fig. A1a, by two plane mirrors separated by a medium whose ray transfer matrix is  $\begin{bmatrix} A & B \\ C & D \end{bmatrix}$  when traversed from left to right. Where an actual resonator mirror is curved, this is represented by a plane mirror and adjacent lens, and the lens is then included in the matrix  $\begin{bmatrix} A & B \\ C & D \end{bmatrix}$ . We assume the resonator contains an aperture of diameter  $2a$ , located at the surface of the right-hand mirror (Fig. A1a) and centred on the resonator axis. The round-trip diffraction loss of this resonator is the same as the single-pass loss of the symmetric resonator in Fig. A1b in which the matrix  $\begin{bmatrix} D & B \\ C & A \end{bmatrix}$  corresponds to the medium in Fig. A1a being traversed from right to left. Thus the overall matrix  $\begin{bmatrix} A' & B' \\ C' & D' \end{bmatrix}$  of the symmetric resonator is  $\begin{bmatrix} A' & B' \\ C' & D' \end{bmatrix} = \begin{bmatrix} A & B \\ C & D \end{bmatrix} \begin{bmatrix} D & B \\ C & A \end{bmatrix} = \begin{bmatrix} 2AD-1 & 2AB \\ 2CD & 2AD-1 \end{bmatrix}$  where we have made use of the relation  $AD - BC = 1$ .

It can be shown (see e.g. Baues [12]) that the diffraction loss of the above symmetric resonator is the same as that of an equivalent empty symmetric resonator having a  $g$  parameter given by  $g = A' = 2AD - 1$  and Fresnel number  $N = a^2/\lambda B' = a^2/2\lambda AB$ . From Equation 16 we write  $g = 2G_1G_2 - 1$  and since  $G_1G_2 = \frac{1}{2}$  for a correctly adjusted dynamic stable resonator it follows that the diffraction losses are the same as those of a symmetric resonator with  $g = 0$ , i.e. a confocal resonator. By substituting from Equations 16 and 17a, the expressions for  $A$  and  $B$  for a telescopic resonator, it is found that the Fresnel number  $N$  of this equivalent resonator is given by

$$N = \frac{a^2}{2\lambda M^2 L' (1 - L'/R_1)} \tag{A1}$$

In the particular case where  $R_1$  is plane this reduces to

$$N = \frac{a^2}{2\lambda M^2 L'} \tag{A2}$$

If the aperture in Fig. A1 had instead been located at the left-hand mirror, then a similar analysis shows that the round-trip diffraction loss would be the same as that of an equivalent symmetric resonator whose Fresnel number is

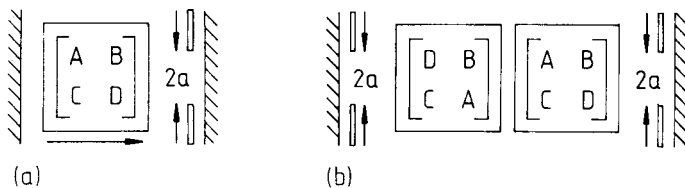


Figure A1 (a) Resonator with plane mirrors with an aperture of diameter  $2a$  adjacent to the right-hand mirror, and separated by an optical medium whose ray-transfer matrix is  $\begin{bmatrix} A & B \\ C & D \end{bmatrix}$  for propagation from left to right. (b) A round trip of the resonator in Fig. A1b, starting from the aperture, and shown as an unfolded resonator.

$$N = \frac{a^2}{2\lambda BD} = \frac{a^2}{2\lambda L'(1 - M^2 L'/R_2')} \quad (\text{A3})$$

Thus, as far as the mode selectivity is concerned, it is immaterial whether the aperture is in the expanded or contracted beam, i.e. at the right-hand or left-hand mirror respectively, provided the aperture size is chosen to give the same value of  $N$  in either case.

## References

1. D. C. HANNA, C. G. SAWYERS and M. A. YURATICH, *Opt. Commun.* **37** (1981) 359–62.
2. C. M. STICKLEY, *IEEE J. Quant. Elect.* **QE-2** (1966) 511–8.
3. J. STEFFEN, J. P. LÖRTSCHER and G. HERZIGER, *ibid* **QE-8** (1972) 239–45.
4. R. B. CHESLER and D. MAYDAN, *J. Appl. Phys.* **43** (1972) 2254–7.
5. J. P. LÖRTSCHER, J. STEFFEN and G. HERZIGER, *Opt. Quant. Elect.* **7** (1975) 505–14.
6. R. L. HERBST, H. KOMINE and R. L. BYER, *Opt. Commun.* **21** (1977) 5–7.
7. D. C. HANNA and L. LAYCOCK, *Opt. Quant. Elect.* **11** (1979) 153–60.
8. G. BRASSART, G. BRET and J. M. MARTEAU, *Opt. Commun.* **23** (1977) 327–9.
9. P. H. SARKIES, *ibid* **31** (1979) 189–91.
10. T. LI, *Bell Syst. Tech. J.* **44** (1965) 917–32.
11. H. KOGELNIK and T. LI, *Appl. Opt.* **5** (1966) 1550–67.
12. P. BAUES, *Opto-Elect.* **1** (1969) 37–44.
13. W. KOECHNER, 'Solid State Laser Engineering', Vol. 1 (Springer Series in Optical Sciences) (Springer-Verlag, Berlin, 1976).
14. R. WOOD, private communication.
15. G. D. BALDWIN and E. P. RIEDEL, *J. Appl. Phys.* **38** (1967) 2726–38.
16. J. P. GORDON, R. C. C. LEITE, R. S. MOORE, S. P. S. PORTO and J. R. WHINNERY, *ibid* **36** (1965) 3–8. (1965) 3–8.
17. L. W. CASPERSON and S. D. LUNNAM, *Appl. Opt.* **14** (1975) 1193–9.